Stochastic variational method for elastic scattering

J. Y. Zhang and J. Mitroy*
ARC Center for Anti-Matter Studies, Faculty of Technology, Charles Darwin University, Darwin NT 0909, Australia
(Received 11 March 2008; published 14 July 2008)

The stochastic variational method is used with a confining potential of the form $V=\lambda r^{12}$ to generate correlated basis sets capable of accurately describing low-energy elastic scattering. Stabilization concepts are then used to extract the phase shifts and other scattering observables. The method is applied to positron scattering from H and He, and Ps scattering from H and He. The results of the calculations are in uniformly good agreement with previous high quality calculations or with experiment. In particular, the scattering length for Ps-He scattering is found to be $1.566a_0$ while the zero-energy ${}_1Z_{\rm eff}$ was 0.1157. The Ps-He s-wave phase shift is found to be incompatible with experimental momentum transfer cross sections obtained by the Doppler broadening technique.

DOI: 10.1103/PhysRevA.78.012703 PACS number(s): 03.65.Nk, 36.10.Dr, 34.90.+q

I. INTRODUCTION

The stochastic variational method (SVM) [1–3], and variants [4–8] have recently become some of the most powerful methods for studying few-body systems. Among the notable applications of the method are the description of small molecules without making the Born-Oppenheimer approximation [7] and the description of atoms with attached positrons [9,10]. The success of the method is based on the analytic properties of the explicitly correlated Gaussian (ECG) [3,4,11,12]. The basis functions have the form

$$G_k = \exp\left(-\frac{1}{2}\sum A_{ij}^k \mathbf{x}_i \cdot \mathbf{x}_j\right), \tag{1}$$

where $\mathbf{x}_i$ is the coordinate of ith particle, The ECG basis functions have the property that the multicenter integrals that occur with correlated basis sets are surprisingly easy to evaluate.

The basic strategy behind the SVM exploits the ease with which the Hamiltonian matrix elements can be evaluated. The wave function is expanded in a linear combination of ECGs,

$$\Psi = \sum_k c_k G_k. \tag{2}$$

The linear parameters are obtained by solving a generalized eigenvalue problem. The optimal set of nonlinear parameters of the ECGs come from an iterative trial-and-error search. One simply adjusts the A_{ij} exponents in a random process and retains those sets of exponents that result in a decrease in the energy.

The SVM had been adapted to perform elastic scattering calculations [13,14] by using stabilization concepts [15,16]. The most important applications of the SVM approach to collision physics were to positronium-atom scattering. The reason for this lies in the technical difficulties associated with performing scattering calculations between two composite objects with internal structure. The multicenter integrals that naturally occur can greatly complicate the evaluation of the scattering Hamiltonian. However, evaluation of the scattering Hamiltonian is straightforward when ECGs are used to describe the scattering wave function.

The present paper describes modifications to the SVM scattering ansatz that leads to a more efficient procedure with improved numerical stability. The method is then used to determine the very low-energy s-wave phase shifts for e^+-H, e^+-He, Ps-H, and Ps-He scattering. In addition, the direct annihilation parameter $Z_{\rm eff}$ is computed for the e^+-H and e^+-He systems. Finally, the pick-off annihilation parameter ${}_1Z_{\rm eff}$ for Ps-He scattering is determined and found to be in reasonable agreement with experiment [17–20].

II. THEORY

The stabilization concept exploits the fact that the radial dependence of a positive energy pseudostate resulting from the diagonalization of the Hamiltonian approximates that of the true continuum wave function over a reasonably wide range. Therefore, if the Hamiltonian is diagonalized in a basis that is capable of describing the interparticle dynamics, then one should expect to get reasonably accurate phase shifts. The problem of course is to construct the basis.

In the SVM stabilization method, the basis is constructed by dividing space into two regions, an inner (or interaction) region and an exterior (or asymptotic) region. In the interaction region there are strong interactions between the projectile and target. The basis for this region is generated by the SVM [13,14]. In the asymptotic region, the wave function is essentially a product of the target ground-state wave function, the projectile ground-state wave function, and a scattering wave function which can be written as $\sin(kR+\delta)$, where R is the distance between the center-of-mass of target and projectile. It is a simple matter to generate a basis of ECGs that is capable of giving a good representation of the continuum wave function in the asymptotic region [13,14].

There are many similarities between the present and previous [13,14] versions of the stabilization SVM. However, some small but significant changes which relate to the manner in which the inner and exterior basis sets are generated have improved its reliability and extended its range of applicability.

*jxm107@rsphysse.anu.edu.au

A. Generation of the inner basis

In the interaction region, the SVM [1,2,10] is used to define an ECG basis (dimension=K) that gives an accurate solution of the Schrödinger equation for the lowest-energy state. This is easy to do in cases where the scattering complex supports a bound state. However, in a number of cases the complex does not support a bound state and so an unconstrained variational minimization would result in a wave function with a very low-energy projectile localized a long distance from the target.

The variational procedure has been modified to prevent this from occurring. In previous work, the exponents β_i of the Gaussians connecting the electron and positron to the nucleus were restricted to be larger than a certain minimum size, say $\alpha_i > 0.001$. This constrained the projectile and target to be localized reasonably close together and gave a SVM iteration procedure that effectively solved the Schrödinger equation in a soft-sided box. However, the projectile and target did exhibit a tendency to drift apart as the optimization is carried out. Further, there is no well defined variational principle involved and this makes it difficult to determine whether the inner basis is giving converged expectation values.

In the present work a confining potential of the form

$$V_C(r) = \lambda r^n, \tag{3}$$

is added to the Hamiltonian. The confining potential acts between the nucleus and the light particles. The use of the confining potential means that the inner basis is generated with a well defined variational procedure with no constraints governing the allowable ranges for the variational parameters (apart from those implicit in ensuring a square integrable basis function). Inclusion of the confining potential meant it was possible to relentlessly drive the inner basis to convergence, something that was difficult to achieve with the parameter constraint approach used previously [13,14].

It should be noted that Guerout *et al.* [21,22] have also investigated the usage of a real confining potential to determine the solution of Schrödinger equation for scattering problems. The confined wave function obtained by adapting quantum chemistry codes was used within a multichannel quantum defect theory formalism to model the transition intensities to the Rydberg and continuum states of NO.

The functional form of $V_C(r)$ was influenced by three factors. First, it was desirable to have a potential that has matrix elements that are easy to evaluate and furthermore has finite matrix elements for an ECG basis. Second, we wish to have a potential that is very small when the projectile and target are close together. Finally, the potential should increase rapidly once r reaches a critical value. The second and third criteria can be satisfied by choosing λ to be small and n to be large. For example, consider the choice $\lambda = 10^{-19}$ and $n=12$. At $r=10$ one has $V_C(r)=10^{-7}$. At $r=16$ one has $V_C(r)=2.8\times10^{-5}$. At $r=30$ one has $V_C(r)=5.3\times10^{-2}$ and the potential is beginning to confine the particles.

B. Generation of the exterior basis

Once the inner wave function has been obtained, a set of ECGs designed to represent a positive energy projectile coupled to the target are added to the basis. The particulars are best explained by reference to a specific example, namely, the Ps-He system.

The Ps and He ground states are represented by a linear combination of ECGs which are constructed by performing a normal bound state SVM calculation. The typical exterior basis function consists of a product of the Ps and He ground state wave functions coupled together with a Gaussian connecting the Ps center-of-mass coordinate to the nucleus. This basis function can be written

$$\Psi^i_{\rm out} = \exp(-\alpha_i R^2)\psi^{\rm Ps}(\mathbf{r}_0 - \mathbf{r}_1)\psi^{\rm He}(\mathbf{r}_2,\mathbf{r}_3), \tag{4}$$

$$\psi^{\rm Ps}(\mathbf{r}_0 - \mathbf{r}_1) = \sum_j c_j F_j^{\rm Ps}(\mathbf{r}_0 - \mathbf{r}_1), \tag{5}$$

$$\psi^{\rm He}(\mathbf{r}_2,\mathbf{r}_3) = \sum_k d_k F_k^{\rm He}(\mathbf{r}_2,\mathbf{r}_3), \tag{6}$$

where R is the distance between the He nucleus and the Ps center-of-mass. The $\psi^{\rm Ps}(\mathbf{r}_0-\mathbf{r}_1)$ and $\psi^{\rm He}(\mathbf{r}_2,\mathbf{r}_3)$ are the Ps and He wave functions written as linear combinations of ECGs ($F_j^{\rm Ps}$, $F_k^{\rm He}$). The exponents of the center-of-mass Gaussians, α_i are generally chosen to form an even tempered sequence.

The difference between this approach and a previous approach [13,23] is that the exterior basis functions are now linear combinations of products of ECGs. In previous calculations, the individual ECGs were treated separately in the final diagonalization giving a more flexible trial wave function. This gave a basis set that is larger in dimension, but more prone to linear dependence problems [13,23]. Linear dependency issues provided the limit on the size of calculation that could be done, and compromises in the size of the basis were made in the earlier treatments of Ps-H and Ps-Ps scattering [14,23].

C. Obtaining the phase shifts and annihilation parameters

The Hamiltonian is diagonalized (with the confining potential omitted) in the full inner plus exterior basis to generate the set of positive energy pseudostates. The phase shifts were derived by a least-squares fit to the overlap of the target and projectile wave functions with the pseudo-states. This is best explained by reference to a specific example. The overlap function $C(R)$ for the Ps-He system is defined as

$$C(\mathbf{R}) = \int d^3r_0 d^3r_1 d^3r_2 d^3r_3 \delta((\mathbf{r}_0+\mathbf{r}_1)/2 - \mathbf{R}) \times \psi^{\rm Ps}(\mathbf{r}_0,\mathbf{r}_1)\psi^{\rm He}(\mathbf{r}_2,\mathbf{r}_3)\Psi(\mathbf{r}_0,\mathbf{r}_1,\mathbf{r}_2,\mathbf{r}_3). \tag{7}$$

A least-squares fit over a finite interval $R\in[R_{\rm in},R_{\rm outer}]$ to a wave function with the asymptotic form $B\sin(kR+\delta_0)$ was used to extract the phase shift for each positive energy pseudostate. The value of $R_{\rm in}$ should be sufficiently large for the projectile and target wave functions to have minimal overlap. Typically $R_{\rm in}$ was about $15a_0$. The value of $R_{\rm outer}$ should lie in the region of space where the probability density region of inner basis is still a reasonable fraction (e.g., 20%) of the peak in probability density. Typically, $R_{\rm outer}$ was between 25 to $30a_0$.

The form of the wave function over $R \in [R_{\text{in}}, R_{\text{outer}}]$ was not a pure sinusoidal form. Actually, $B \sin(kR+\delta_0)$ is evaluated at $R=500a_0$ and then a numerical integration inwards is done in the presence of the dominant long range field. In the case of a positron-atom complex, this is $-\alpha_d/(2r^4)$ where α_d is the polarizability of the atom. In the case of a Ps-atom complex, the dominant term is $-C_6/R^6$ where C_6 is the dispersion constant between the Ps and atomic ground states [24,25].

In addition to the phase shift, it is also necessary to determine the direct and pick-off annihilation rates. The direct annihilation rate describes annihilation during positron-atom or positron-molecule collisions and is usually expressed in terms of Z_{eff}. The parameter Z_{eff} is defined as

$$Z_{\text{eff}} = \sum_i \int d^3r_0 d^3x \delta(\mathbf{r}_i - \mathbf{r}_0) |\Psi(\mathbf{x}, \mathbf{r}_0)|^2. \quad (8)$$

Here $\Psi(\mathbf{x}, \mathbf{r}_0)$ is the total wave function of the system, $\mathbf{r}_0$ is the positron coordinate, while $\mathbf{x}=\{\mathbf{r}_1, \mathbf{r}_2, \ldots\}$ is the collective set of electron coordinates. Z_{eff} is equal to the number of target electrons when the continuum positron wave function is a plane wave. The definition of Z_{eff} implicitly accounts for spin averaging.

Pick-off annihilation describes the quenching of *ortho*-Ps by collisions with a gas. When positrons are injected into an atomic or molecular gas they are subjected to a complex sequence of elastic, inelastic and annihilating collisions [26,27]. Eventually they slow down sufficiently so that no further excitations are possible. After a sufficiently long time, the dominant species left in the gas is *ortho*-Ps [26–28]. The *ortho*-Ps state decays via the 3γ process with an annihilation rate of 7.04×10^6 s^{-1} which is about 1000 times slower than the para(singlet)-Ps decay. In addition to its own intrinsic decay, *ortho*-Ps can collide with the atoms (molecules) of the gas and the positron can annihilate with the atomic (molecular) electrons.

The pick-off annihilation parameter, namely, ${}_1Z_{\text{eff}}$, is derived from experiment using the identity [29]

$$\lambda_p = \lambda_{ortho\text{-Ps}} + 0.804 n\, {}_1Z_{\text{eff}}. \quad (9)$$

In this equation, λ_p is the decay rate directly measured from experiment, $\lambda_{ortho\text{-Ps}}$ is the decay-rate of *ortho*-Ps, and n is the gas density in amagat. Variation of the gas density permits the determination of ${}_1Z_{\text{eff}}$.

Calculation of the pick-off parameter requires the evaluation of the overlap matrix element between all the positron-electron pairs in a singlet spin state for a total wave function that is in a triplet spin state. It can be written as [29]

$${}_1Z_{\text{eff}} = \sum_i \int d^3r_0 d^3x O_S(i,0) \delta(\mathbf{r}_i - \mathbf{r}_0) |\Psi(\mathbf{x}, \mathbf{r}_0)|^2. \quad (10)$$

Here $\Psi(\mathbf{x}, \mathbf{r}_0)$ is the Ps-scattering wave and $O_S(i,0)$ is a projection operator that ensures only electron-positron pairs (electron i) in a spin singlet state annihilate. It only makes sense to talk of pick-off annihilation for closed shell targets, since the much larger exchange quenching occurs for open-shell targets [30]. In the plane wave Born approximation, ${}_1Z_{\text{eff}}$ reduces to $\frac{N}{4}$, where N is the number of closed shell electrons [31].

The present calculation of the phase shifts and scattering length is best described as quasivariational. Although, no formal minimum principle applies, the tendency is for the derived scattering length to decrease as the basis optimization drives down the energy in the inner region.

D. Representation of the target wave function

In an initial series of calculations on the e^+-He system it was found that the phase shift and annihilation rate were sensitive to the quality of the helium wave function used in the exterior basis. The scattering length showed no signs of convergence and continually increased as the dimension of the inner basis was increased. This occurred when a relatively small dimension wave function was being used to represent the He ground state in the exterior basis. The salient point proved to be position of the $E=0$ threshold energy. This is effectively determined by the energy of the helium ground state wave function as given by the finite basis wave function.

The phase shift is sensitive to the difference between the potential in the interaction and exterior regions. Assuming an attractive potential in the interaction region, the usage of a poor He ground wave function leads to the local energy in the asymptotic region being too large. This resulted in phase shifts which were simply too large.

The solution to the problem was to simply use a better wave function for the helium ground state. This required the use of SVM wave functions with a ECG basis of dimension 40 or larger.

E. On determining the phase shift from the density

The phase shifts obtained in this work were all obtained by computing overlap functions involving the projectile and target ground states. This did increase program complexity. A simpler alternative would be to extract the phase shifts from the density of one of the particles. In the case of the e^+-H(He) systems, one computes the positron density and then a fit to $D \sin^2(kR+\delta_0)$ can be used to get D and δ_0. In the case of Ps-H(He) scattering, the positron density can be taken as a surrogate of the Ps density and once again a fit to $D \sin^2(kR+\delta_0)$ can be used to set the overall normalization of the wave function in addition to the phase shift.

One feature of the SVM stabilization approach is the presence of fluctuations in the phase shift or Z_{eff} [13,23]. In the case of the present work, the fluctuations were most noticeable for the e^+-He system which has relatively small phase shifts. The size of these fluctuations were always larger when the phase shifts were extracted by fitting to the density, as opposed to the wave function projection. The density can be used to give reasonable estimates of the phase shift, but determining the phase shifts from a wave function projection is better.

III. POSITRON SCATTERING FROM HYDROGEN

The first test of the ability of the new stabilization SVM was for the e^+-H system. The inner basis dimension was 360

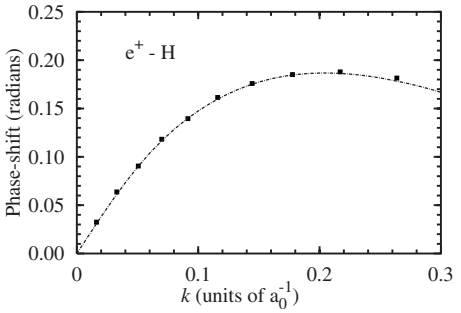

FIG. 1. The s-wave phase shift δ_0 for e^+-H scattering as a function of k (units of a_0^{-1}). The solid line represents a continuous fit to the phase shifts taken from a large scale close coupling calculation [32] which gives phase shifts that are about 0.5% below the close to exact values of Bhatia *et al.* [33].

and was generated with the confining potential $V_C(r)=6.0\times10^{-20}r^{12}$. The mean radius of the positron in the confining potential was $14.8a_0$.

The exterior basis consisted of 35 positron Gaussians (defined by the relation $\alpha_i=19.54/1.45^{i-1}$) multiplying the hydrogen ground state wave function. The H ground state was written as a linear combination of 10 ECGs which gave a binding energy of −0.499999318 a.u. The presence of the confining potential had hardly any effect on the binding energy of the H ground state, and only resulted in changes in the twelfth and subsequent digits of the energy. The region $r\in[16,27]a_0$ was used for the stabilization fit. The outer limit of $27a_0$ was chosen to reduce the size of the fluctuations in the two phase shifts with the lowest energy.

The s-wave phase shift and annihilation parameter are depicted in Figs. 1 and 2. The random fluctuations that seem to be inherent with the stabilization approach are just noticeable.

The scattering length, A was determined by fitting the phase shifts with $k<0.20a_0^{-1}$ to an expression from modified effective-range theory [34–36]. The expression is

$$k\cot\delta(k) = -\frac{1}{A} + \frac{\alpha_d\pi k}{3A^2} + \frac{2\alpha_d k^2}{3A}\ln\left(\frac{\alpha_d k^2}{16}\right) + Bk^2 + Ck^3, \tag{11}$$

where $\alpha_d=4.5a_0^3$ is the polarizability of the hydrogen ground state. The resulting value of the scattering length was

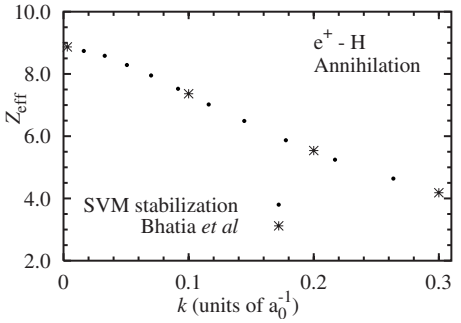

FIG. 2. The s-wave annihilation parameter $Z_{\rm eff}$ for e^+-H scattering as a function of k (units of a_0^{-1}).

TABLE I. The scattering length and $Z_{\rm eff}(k=0)$ (experimental values for helium are at thermal energies).

Method	A (units of a_0)	$Z_{\rm eff}^{(0)}$
	Hydrogen	
Present SVM	−2.094	8.75
Kohn-variational [37,41]	−2.1036	8.868
	Helium	
Present SVM	−0.474	3.955
Kohn-variational [45]	−0.50	3.932
Experiment		3.89 ± 0.04[17]
		3.94 ± 0.02[28]
		3.86 ± 0.04[18]

$-2.094a_0$. This is within 1% of the close to exact value of $-2.1036a_0$ [37].

A fit using the expression

$$Z_{\rm eff}(k) = Z_{\rm eff}^{(0)} + Z_{\rm eff}^{(1)}k^2 + Z_{\rm eff}^{(2)}k^4, \tag{12}$$

was made to the values of $Z_{\rm eff}$ with $k<0.15a_0^{-1}$. The effective range expansion for $Z_{\rm eff}$ does not have any terms proportional to k [38]. The fit gave a zero-energy annihilation rate of $Z_{\rm eff}^{(0)}=8.75$. This value is only 1.2% smaller than the close to exact value of 8.87 [37]. The threshold values of the scattering parameters are summarized in Table I.

IV. POSITRON SCATTERING FROM HELIUM

The ability of the stabilization SVM to describe more complicated systems was tested in a calculation of s-wave e^+-He scattering. The inner basis dimension was 1000 and was generated with the confining potential $V_C(r)=3.2\times10^{-19}r^{12}$. The mean radius of the positron for the final converged basis was $13.6a_0$. The outer basis consisted of 35 positron Gaussians, defined by the relation $\alpha_i=19.54/1.45^{i-1}$, multiplying the He ground state wave function. The basis dimension for the He ground state was 50 and the energy of this state was −2.90372295 a.u. (the exact He energy is −2.90372438 a.u. [39]). The energy of the He ground state in the field of the confining potential was increased by less than 10^{-14} Hartree. The annihilation parameter was stable to better than 0.1% against further enlargement of the dimension of the He ground state. The stabilization fit was performed over the interval $R\in[15,26]$ a_0. A value of $1.3832a_0^3$ [40] was adopted for the He polarizability.

There is some uncertainty in the existing values of the positron-helium s-wave phase shifts that mainly relate to the description of the helium ground state. The use of inexact wave functions is known to cause problems in variational calculations [41–44]. The calculations can be divided into two classes, those that use a helium ground state wave function of roughly Hartree-Fock quality [41,42], and those that use a Hylleraas wave function to describe the helium ground state [43,44].

Figure 3 shows the present calculation of the s-wave phase shift. The stabilization fluctuations of ±0.003 rad are

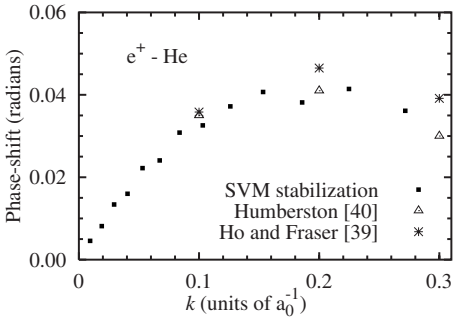

FIG. 3. The *s*-wave phase shift for e^+-He scattering as a function of k (units of a_0^{-1}). Data points from the variational calculations of Ho and Fraser [42] and the H22 calculation of the Humberston group [43] are also shown.

noticeable since the phase shifts are so small. A scattering length of $-0.474a_0$ was obtained by fitting Eq. (11) to the phase shifts satisfying $k<0.20a_0^{-1}$.

Figure 3 also shows phase shifts taken from some earlier variational calculations. The calculation of Ho and Fraser [42] (using their HF2 He ground state) is taken as representative of calculations that use a Hartree-Fock quality wave function for the He ground state. The phase shifts computed with the 22-term Hylleraas ground state [43] by Humberston and co-workers are also depicted in Fig. 3. The present SVM phase shifts are compatible with the phase shifts of Humberston [43]. While Humberston did not report a scattering length, it is possible to deduce a scattering length of $-0.50\pm0.02a_0$ from the tabulated phase shift of 0.035 ± 0.01 rad at $k=0.1a_0^{-1}$ [43].

Figure 4 shows the SVM calculation of $Z_{\text{eff}}(k)$ and compares the results with the Kohn variational calculation of van Reeth and Humberston [45]. Threshold values of Z_{eff} are given in Table I. The agreement between the two calculations is between 1% and 3%. The threshold Z_{eff} for a three-term effective range expansion using Eq. (12) for $k\in[0,0.30]a_0^{-1}$ was 3.955. This is within 1% of the Kohn-variational value of 3.932 [45]. The graphed Kohn-variational Z_{eff} was taken from a polynomial fit to the calculated values. It should be noted that the Kohn-variational polynomial fit had a term linear in k [45], but effective range theory suggests that such a term is not possible [38]. The present values of Z_{eff} are

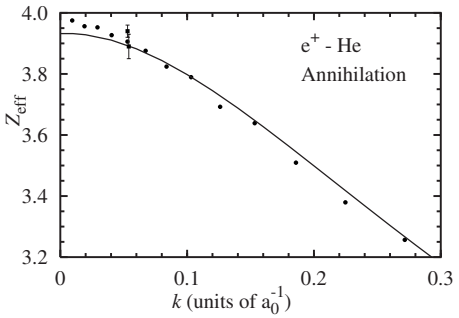

FIG. 4. The *s*-wave annihilation parameter Z_{eff} for e^+-He scattering as a function of k (units of a_0^{-1}). The solid line shows the complex-Kohn calculation [45] while the points with the error bars are experimental [17,28].

marginally larger than the Kohn variation values for $k<0.08a_0^{-1}$ and marginally smaller for $k>0.10a_0^{-1}$.

Two experimental values of Z_{eff} at thermal energies are 3.89 ± 0.04 [17] and 3.94 ± 0.02 [28]. The SVM stabilization value of Z_{eff} is compatible with both of these values.

V. POSITRONIUM SCATTERING FROM HYDROGEN

The description of Ps-H scattering is technically demanding despite the system only having four particles. It is necessary to solve the Schrödinger equation for the scattering of two composite objects, each with their own center of symmetry and allowing for the possibility of exchange between the target electron and the electron that is part of *ortho*-Ps.

The positronium-hydrogen system has two different symmetries which depend on the spin state of the two electrons. The electron-spin singlet actually has a bound state with a total energy of −0.7891968 a.u. [46]. The electron-spin triplet does not have a bound state.

Recent developments [13,14,47–49] have resulted in calculations that can correctly describe most of the dynamical features of Ps-H scattering in the low-energy region. The first of these calculations used the SVM stabilization method [14]. The size of this earlier SVM calculation [14] was limited by linear dependence issues and the dimension of interaction region basis for the electron-spin triplet configuration was only 350. Of the other calculations, the most precise is the (complex) Kohn variational calculation [49]. The *R*-matrix calculation had a channel space including 14 H-type states and 14 Ps-type states [48]. Finally a quantum Monte Carlo (QMC) of *s*-wave scattering has also been reported [47].

The inner basis for the singlet symmetry had a dimension of 1000 ECGs and gave a PsH ground-state energy of −0.7891966. The inner basis for the triplet symmetry had a dimension of 900 and was generated in the confining potential $V_C(r)=5.0\times10^{-20}r^{12}$. The mean radius of the positron was $15.2a_0$.

The exterior basis for both symmetries consisted of 35 functions constructed from products of the Ps and H fragments with the connecting Gaussians specified by the relation $\alpha_i=19.54/1.45^{i-1}$. The Ps ground state was represented by a linear combination of 10 ECGs with an energy of −0.249999665 Hartree. The H ground state was represented by a linear combination of 10 ECGs with an energy of −0.499999318 Hartree. A value of $C_6=34.79$ a.u. [25] was adopted for the Ps-H dispersion coefficient. The stabilization fit was performed over the interval $R\in[16,29]$.

The singlet and triplet phase shifts for the individual pseudostates are plotted in Fig. 5. Also shown are effective range fits (using pseudostates with $k<0.30a_0^{-1}$) to the expression

$$k\cot\delta(k)=-\frac{1}{A}+\frac{1}{2}r_0k^2+Bk^3. \tag{13}$$

The presence of a van der Waals interaction between Ps and H does lead to $O(k^3)$ terms in the effective range expansion. The influence of this term and all other higher order terms on the cotangent of the phase shift are absorbed in the empirical Bk^3 term.

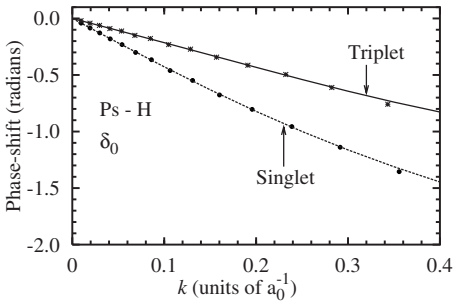

FIG. 5. The s-wave phase shifts (modulo π) for Ps-H scattering as a function of k (units of a_0^{-1}). Phase shifts are shown for both the singlet and triplet electron-spin configurations. The lines represent effective range fits to the phase shifts using Eq. (13).

The derived values of the Ps-H scattering lengths are listed in Table II and compared with the other high quality calculations of Ps-H scattering. The results of five independent calculations give singlet scattering lengths that agree to within 2%. The most accurate of the scattering lengths listed in Table II is that of the Kohn variational calculation [49] and the SVM scattering length agrees with the Kohn value to better that 1%. Examination of the effective range, r_0 reveals a greater spread of values. This is not surprising, since r_0 will be sensitive to the inclusion of additional terms in the effective range expansion (all the fits apart from the present one only have two adjustable parameters) and also to the range of momentum over which the fit is carried out.

There is a larger spread (of about 8%) between the triplet channel scattering lengths listed in Table II. But significantly, the present SVM scattering length of $2.126a_0$ and the complex Kohn variational scattering length of $2.126a_0$ [49] are in perfect agreement (the agreement to an extreme accuracy of better than $0.001a_0$ does have an element of luck). The small R-matrix estimate of the scattering length, namely, $2.06a_0$ [48] would therefore seem to be an aberration. The previous SVM scattering length of $2.22a_0$ [14] should be regarded as being superseded by the present calculation. The QMC calculation gave $A=2.23a_0$ which is about 5% different from the value of $A=2.126a_0$ given by the complex Kohn calculation [49]. While QMC phase shifts are potentially very accurate, uncertainties in defining the nodal surfaces can lead to errors [47,50].

A calculation of Ps-H scattering in the triplet channel has also been performed in the fixed core SVM (FCSVM) [31]. The scattering length was $2.19a_0$. The main source of uncertainty in this calculation was the exact specification of the polarization interactions of the electron and positron in the positronium projectile with the frozen hydrogen ground state. The scattering length in Table II was computed with a cutoff parameter that was tuned to an average value with respect to polarization potentials that reproduce positron-hydrogen and electron-hydrogen (triplet channel) scattering [31].

TABLE II. The scattering length A, and effective range r_0 for the Ps-H system. The numbers in brackets for the QMC calculations represent the statistical uncertainty in the last digits.

Method	A (units of a_0)	r_0 (units of a_0)
Electron-singlet channel		
Present SVM	4.339	2.198
QMC [47]	4.375(34)	2.228(50)
R-matrix [48]	4.41	2.19
Kohn [49]	4.311	2.27
Previous SVM [31]	4.34	2.39
Electron-triplet channel		
Present SVM	2.126	2.385
QMC [47]	2.246(50)	1.425(43)
R-matrix [48]	2.06	1.47
Kohn [49]	2.126	1.39
FCSVM [31]	2.19	1.35
Previous SVM [31]	2.22	1.29

VI. POSITRONIUM SCATTERING FROM HELIUM

A. Calculation details

The extra electron in the helium target makes the description of Ps-He scattering a much more formidable proposition than Ps-H scattering. It would be fair to say that a fully *ab initio* calculation of the Ps-He system is almost an order of magnitude more demanding than the Ps-H calculation. With the exception of a QMC calculation [47], an R-matrix calculation [51], and a T-matrix calculation [52] most of the calculations of the system have been performed using a frozen helium target [13,31,53–57]. An additional observable for helium is the pick-off annihilation rate. Despite being one of the standard observables extracted from positron annihilation experiments [27,58], there has never been a first principles calculation of ${}_1Z_{\rm eff}$ for any physical system that is expected to be accurate to within a factor of 2.

Most previous calculation of Ps-He pick-off annihilation used scattering Hamiltonians based on a frozen He target [31,53–55]. The only fully *ab initio* calculations of Ps-He scattering which relaxed the frozen core approximation [47,51,52] did not determine ${}_1Z_{\rm eff}$. While model polarization potentials can be used to incorporate the impact of the correlations between projectile and target on the phase shift [13,57], short-range correlations have a major impact upon the δ-function expectation value [10,59–62]. Calculations of positron interactions that use model potentials will underestimate the direct and pickoff annihilation rates unless the δ-function matrix element is multiplied by an enhancement factor [60,62].

The actual details of the calculation of Ps-He scattering were as follows. The inner basis had a dimension of 1600 and was generated in the confining potential $V_C(r)=3.2\times10^{-19}r^{12}$. The mean radius of the positron was $13.0a_0$.

The Ps ground state was represented by a linear combination of 9 ECGs with an energy of −0.2499991 Hartree. The helium wave function was written as a linear combination of 45 ECGs and had an energy of −2.90372244 a.u.. The exterior basis consisted of 35 functions constructed from products of the Ps and He fragments with the connecting Gaussians specified by the relation $\alpha_i=19.54/1.45^{i-1}$. The wave

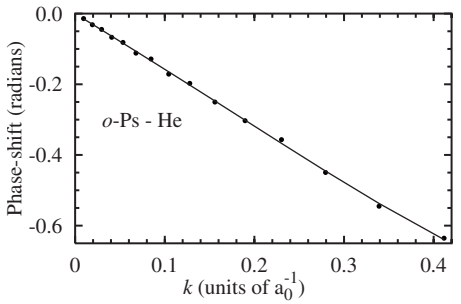

FIG. 6. The *s*-wave phase shift for Ps-He scattering as a function of k (units of a_0^{-1}). The effective range fit to the phase shifts using Eq. (13) is shown as the solid line.

function is of course constructed with due consideration to antisymmetry. A value of $C_6=13.37$ a.u. [25] was adopted for the Ps-He dispersion coefficient. The stabilization fit was performed over the interval $R\in[15,30]$.

B. Effective range fits to the results

The *s*-wave phase shifts resulting from the stabilization calculation are plotted in Fig. 6. The least-squares fit to the effective range expansion (13) for $k<0.4a_0^{-1}$, gave a scattering length of $1.566a_0$ (the statistical uncertainty associated with the fit was about $0.006a_0$). The net decrease in the scattering length when the inner basis was increased in dimension from 1200 to 1600 ECGs was only $0.03a_0$, this is suggestive of an overall level of convergence of about 1%.

The variation of the pick-off annihilation rate ${}_1Z_{\rm eff}$, as a function of k is shown in Fig. 7. The zero-energy value of the annihilation rate was determined from a least-squares fit using the effective range expansion [38]

$$ {}_1Z_{\rm eff}(k) = {}_1Z_{\rm eff}^{(0)} + {}_1Z_{\rm eff}^{(1)}k^2, \tag{14}$$

for $k<0.30a_0^{-1}$. The value of ${}_1Z_{\rm eff}^{(0)}$ for the largest calculation was found to be 0.1157 while ${}_1Z_{\rm eff}^{(1)}$ was −0.0346. The net increase in ${}_1Z_{\rm eff}^{(0)}$ when the basis was increased from 1200 to 1600 was 0.003. However, calculations on the similar triplet state of the Ps-Li^+ bound state revealed that the pick-off rate was one of the most slowly converged expectation values. So it is not possible to absolutely guarantee that ${}_1Z_{\rm eff}$ is converged to better than 10%. The present ${}_1Z_{\rm eff}^{(0)}$ is compared

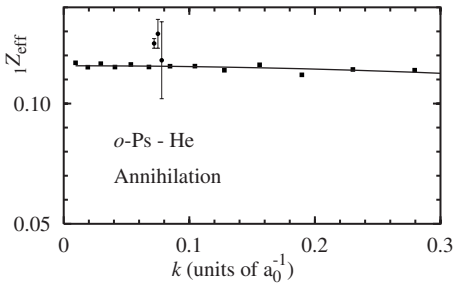

FIG. 7. The *s*-wave pickoff annihilation parameter for Ps-He scattering as a function of k (units of a_0^{-1}). The solid line is the fit to the data using effective range theory while the data points with the error bars are experimental [17,20,28].

TABLE III. Scattering length, effective range, and ${}_1Z_{\rm eff}(k=0)$ for the Ps-He system.

Method	A (units of a_0)	r_0 (units of a_0)	${}_1Z_{\rm eff}^{(0)}$
QMC [47]	1.405		
R-matrix [56]	1.822		
R-matrix [51]	1.60		
FCSVM [31]	1.568	0.914	0.0378
Experiment			0.125 ± 0.002[28]
	1.46 ± 0.08 [17]		0.129 ± 0.006[17]
			0.118 ± 0.016[20]
			0.116 ± 0.004[18]
	1.50 [19]		
	1.49 [63]		
	1.42 [64]		
	1.77 ± 0.25 [65]		
	1.51 ± 0.18 [66]		
	$1.18^{+0.3}_{-0.4}$ [67]		
Present SVM	1.566	2.133	0.1157

with experimental data and other calculations in Table III.

C. Comparisons with other work

The experimental difficulties in measuring the Ps-He cross section has resulted in a wide variance between the different estimates of the low-energy cross section [17,19,65,68]. Accordingly, experiments cannot be used to directly assess the quality of the SVM scattering length. However, ${}_1Z_{\rm eff}$ has been extracted from the γ-decay spectrum by a number of groups [17–20]. The most careful experiment reported a ${}_1Z_{\rm eff}$ value with a stated precision of about 2%, namely, 0.125 ± 0.002 [28]. However, this value of ${}_1Z_{\rm eff}$ was determined by fitting Eq. (8) with a value of $\lambda_{ortho\text{-Ps}}$ that was 3% larger than the most modern estimates of $\lambda_{ortho\text{-Ps}}$. It is possible that the stated precision of 2% is a bit optimistic.

Scattering lengths from a number of earlier calculations are listed in TableIII. The *ab initio* QMC calculation [47] gave a scattering length of $1.405a_0$ and did not give ${}_1Z_{\rm eff}$. A good indicator of the accuracy of the QMC scattering length comes from the examination of the Ps-H scattering lengths in the electron-spin triplet channel. As noted earlier, the QMC calculation gave a scattering length that was 5% larger than the present SVM and previous Kohn variational [49] scattering lengths. A 5% error for the dynamically similar Ps-H system suggests a slightly larger uncertainty for Ps-He. The most likely reason for the discrepancy with the present scattering length of $1.566a_0$ lies in the definition of the nodal surfaces [47,50].

The fixed core stochastic variational method calculation (FCSVM) [31] estimate of the scattering length was $A=1.568a_0$. The FCSVM calculation was also performed using the stabilization approach. The correlations between the Ps constituents and the He ground state [31] were modeled with semiempirical polarization potentials. There is some uncertainty in the exact value of the FCSVM scattering length

due to the ambiguity in the details of the polarization potentials which were determined by reference to $e^{\pm}$-He scattering calculations. The range of allowable scattering lengths was identified as between 1.482 and $1.625a_0$ [31]. The present SVM scattering length lies within this range.

The level of agreement of the FCSVM Ps-H and Ps-He scattering lengths with the present *ab initio* calculations is quite reasonable. This gives added confidence to FCSVM estimates of the scattering lengths for Ps-Ne and Ps-Ar scattering [31].

However, the FCSVM gives a pick-off annihilation rate of $_1Z_{\rm eff}^{(0)}=0.0378$ that is much too small. This gives conclusive proof that the short-range electron-positron correlations included in the fully correlated SVM wave function are necessary for the correct prediction of the pickoff annihilation rate.

Other calculations of the low-energy cross section, and in some case $_1Z_{\rm eff}$ exist [53–56,69,70]. But none of these calculations treat the near threshold region with the same level of technical sophistication as the present SVM calculation or the calculations discussed in the previous two paragraphs [31].

The FCSVM $_1Z_{\rm eff}$ can be bought into closer agreement with experiment by multiplication with an enhancement factor [62]. The enhancement factor may be evaluated in a variety of ways, but is essentially the ratio of the exact annihilation rate divided by an annihilation rate calculated by simply multiplying the electron and positron densities. One enhancement factor of 2.92 was determined by a model potential analysis of e^+-He scattering; the annihilation rate of the model potential wave function was scaled to give the annihilation rate from the Kohn variational calculation [62,71]. Another value of 2.75 was obtained from a constrained basis calculation of the e^+-He system; the annihilation rate was evaluated with the full correlated wave function and also using just the product of the electron and positron densities [62]. Using the improved e^+-He wave function of the present work increases the enhancement factor to 2.84. Finally an enhancement factor of 2.67 was obtained from the present Ps-He wave function by taking the ratio of the exact pick-off annihilation rate with the value determined by multiplying the positron density with the electron density of the He ground state. Using these three enhancement factors with the FCSVM $_1Z_{\rm eff}$ of 0.0378 results in values that range from 0.101 to 0.110. The overall accuracy of 10–20 % is reasonable.

The energy dependence of the *s*-wave part of $_1Z_{\rm eff}$ is one of decreasing pick-off annihilation as energy increases. The actual rate of decrease is very small, and at $k=0.3a_0^{-1}$ the decrease from the zero-energy value was only 3%. This is almost the same as the energy decrease in the FCSVM calculation with a scattering length of $1.568a_0$ [31]. This indicates the enhancement factor for pick-off annihilation has a slow variation with energy near the $E=0$ threshold. Experimentally the pick-off annihilation rate has been measured in two experiments to increase with increasing temperature [17,72] and in one experiment to decrease with increasing temperature [73]. The resolution of this conundrum will probably require a first principles calculation of the *p*-wave behavior of $_1Z_{\rm eff}$.

D. The momentum transfer cross section

The scattering length of $1.566a_0$ implies that the zero-energy cross section should be 9.81 πa_0^2. One class of experiments examined the thermalization of *ortho*-Ps in gas phase experiments to give estimates of the very low-energy momentum transfer cross section. In terms of phase shifts, the momentum transfer cross section is defined

$$\sigma_m=\sum_{l=0}^{\infty}\frac{4(l+1)}{k^2}\sin^2(\delta_{l+1}-\delta_l) \tag{15}$$

The estimates of the zero energy cross section are $8.4\pm0.5\pi a_0^2$ by Canter *et al.* [17], 9.0 πa_0^2 by the University College London group [19], and $12.5\pm3.4\pi a_0^2$ by the Tokyo group [65]. The momentum transfer cross section of $2.6\pm0.5\pi a_0^2$ by the Michigan group [68] was obtained at slightly higher energies [68]. Most recently, an energy-dependent cross section given by $\sigma_m=4.9-13.5E+8.5E^2$ was derived by the Wisconsin group [67]. In this expression, the cross section is in Å^2 and the energy is in eV. It should be noted that there is a good deal of uncertainty in the Wisconsin group cross section at $E=0$. The actual data measured by the Wisconsin group correspond to an energy greater than 0.50 eV, and the use of a momentum transfer cross section with a quadratic form to extrapolate their cross section to $E=0$ is a major source of uncertainty. The energy dependence of the low-energy cross section would be best described using effective range theory [74,75], and the quadratic form adopted by the Wisconsin group is of questionable accuracy [67].

Estimates of the scattering length have been obtained from the analysis of *ortho*-Ps annihilation in liquid helium and high density gaseous helium [17,63,64,66,76]. These model-dependent estimates are generally slightly smaller than the present scattering length. Estimates of the scattering length include $1.49a_0$ [63], $1.42a_0$ [64], and $1.51\pm0.18a_0$ [66].

The present *s*-wave phase shift was used to construct a momentum transfer cross section by making reference to a published *R*-matrix elastic cross section for the *P*-wave [51] and using a long range analysis to estimate the *D*-wave cross section. The *R*-matrix calculation included seven Ps states and seven He states. The *R*-matrix phase shifts were deduced by digitizing the published partial wave elastic cross sections and then converting them to phase shifts [51].

The *R*-matrix *s*-wave phase shift is not much different from the present phase shift. The *R*-matrix scattering length was $1.60a_0$ which is only 2% larger than the present scattering length.

The *p*-wave phase shift was digitized after assuming the phase shift was negative. The Ps-He *p*-wave phase shift is expected to be similar to the *p*-wave phase shift for Ps-H scattering in the electron spin-triplet configuration and this phase shift is known to be negative [14,51]. After digitization, the phase was then fitted to an empirical fitting formula based on effective range theory, *viz.*

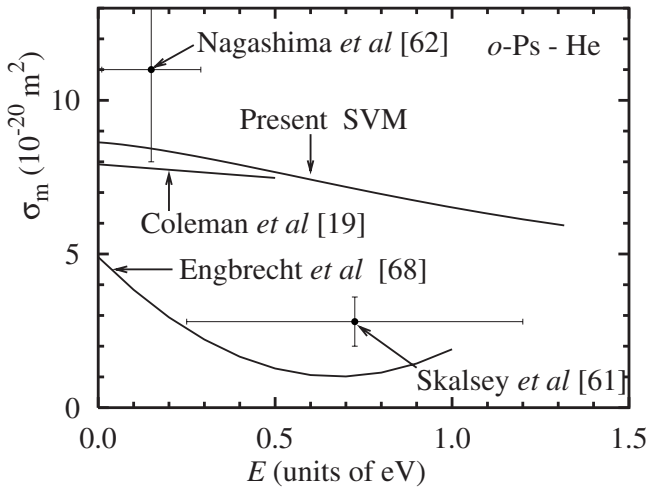

FIG. 8. The momentum transfer cross section for Ps-He scattering (units of 10^{-20} m^2) as a function of E (units of eV). The horizontal error bars shown with some of the experimental data indicate the energy range used in the determination of the momentum transfer cross section.

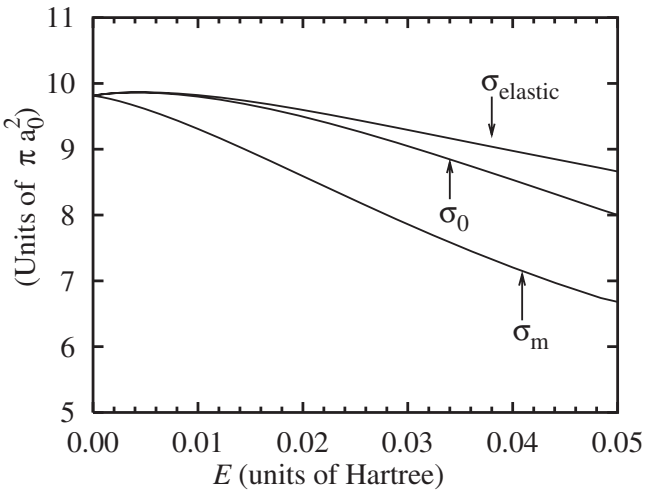

FIG. 9. The total cross section $\sigma_{elastic}$, the momentum transfer cross section σ_m, and the s-wave partial elastic cross section for Ps-He scattering (all in units of πa_0^2) as a function of E (units of Hartree).

$$\tan(\delta_2) = -Ak^3 + Bk^5 + Ck^7. \tag{16}$$

Values of $A=1.0$ a.u. and $B=-2.4$ a.u. and $C=8.4$ a.u. were chosen. This expression neglects a k^4 term arising from C_6 [77–79], but C_6 is quite small and the impact it does have will be partly compensated by the k^5 and k^7 terms.

The lowest order term in the d-wave phase shift comes from the C_6/r^6 van der Waals interaction. The lowest order term in the expression for the phase shift can be evaluated via perturbation theory [77–80]. It is

$$\tan(\delta_2) \approx \frac{12\pi C_6 k^4}{945}, \tag{17}$$

where $C_6=13.37$ a.u. [25]. At $k=0.4a_0^{-1}$ this expression gives $\delta_2=0.0137$ rad. Short range effects for the d-wave are repulsive [52,81].

The composite momentum transfer cross section calculated from the present s-wave phase, the digitized and fitted R-matrix p-wave phase, and Eq. (17) for the d-wave phase is plotted and compared with various experimental values in Fig. 8. This composite cross section is compatible with the rough estimate of the momentum transfer cross section given by Coleman *et al.* [19]. However, the composite cross section is incompatible with those of Skalsey *et al.* [68] and the Wisconsin group *et al.* [67] which use the Doppler broadening technique. In fact, it is absolutely impossible to reconcile the current s-wave phase shift with either of the Doppler broadening derived cross sections at $E=0.6$ eV ($k\approx 0.3a_0^{-1}$). At this energy, the d-wave phase shift can be neglected and the momentum transfer cross section reduces to

$$\sigma_m \approx \frac{4\pi}{k^2}[\sin^2(\delta_0 - \delta_1) + 2\sin^2(\delta_1)]. \tag{18}$$

The s-wave phase shift is $\delta_0=0.480$ rad. The absolute minimum value that σ_m can achieve is $6.7\pi a_0^2$ for a p-wave phase shift of $\delta_1=-0.15$ rad. Any other value of δ_1 will result in a larger momentum transfer cross section. Although the Wisconsin group state that their cross section is consistent with other experiments that have a zero energy cross section of $\approx 10\pi a_0^2$, this statement should be given little weight since the quadratic form they use to describe the energy dependence of the momentum transfer cross section is not founded in effective range theory [74,75].

Both the Skalsey *et al.* and the Wisconsin group *et al.* experiments use the Doppler broadening of the annihilation γ-ray spectrum to deduce the momentum transfer cross section (other approaches have looked at the angular correlation of the annihilation radiation [19,65]). The analysis of the Doppler broadening data is quite complicated, and it is possible that there are invalid assumptions in the extraction of the cross section from the raw data.

Finally, Fig. 9 shows the elastic and momentum transfer cross sections as a function of energy up to 0.05 Hartree. The $L=0$ partial cross section, σ_0 is also depicted. The elastic cross section is dominated by the $L=0$ partial cross section for the energy range shown. The cancellation between the s and p wave phase shifts causes the momentum transfer cross section to be about 30% smaller than the elastic cross section at $E=0.05$ Hartree.

VII. CONCLUSION

To summarize, an improved version of the SVM stabilization ansatz has been developed and used to describe the close to threshold scattering of four systems, namely, the e^+-H, e^+-He, Ps-H, and Ps-He systems. The results on the e^+-H and e^+-He systems can be regarded as validation exercises that demonstrate the ansatz is capable of achieving 1–2 % accuracy for both the phase shifts and annihilation rate. One positive aspect of the present approach is that the linear dependence problems associated with the method seem to be have been largely eliminated [23]. The other improvement relates from the use of the confinement potential.

The inner basis could be systematically improved since a well defined variational principle was in operation

One advantage of the method lies in its ability to treat positronium scattering since this type of projectile is difficult to treat by other methods. The comparison with the Kohn scattering lengths for Ps-H scattering suggest that the low energy *s*-wave phase shifts are now known with an accuracy of about 1%.

The results for the Ps-He system represent an *ab initio* determination of the scattering length that has an accuracy of about 1–2 %. A previous *R*-matrix calculation gave a scattering length only 2% larger than the present calculation [51]. The authors of the *R*-matrix calculation did not make any statements about the overall level of accuracy of their phase shifts, possibly due to approximations in their representation of the ground and excited states of the He target. So the two most sophisticated *ab initio* calculations of Ps-He now give consistent results. The level of agreement between the calculated and experimental pickoff annihilation rates gives confidence that the present SVM calculation has captured most of the physics necessary to describe low-energy Ps-He scattering.

One future application of the method would be to extend it to encompass *p*-wave scattering. This would permit a more precise evaluation of the momentum transfer cross section. Further, it would permit a definitive description of the energy dependence of ${}_1Z_{\mathrm{eff}}$ below 1–2 eV incident energy. Another extension would involve the description of Ps-H_2 scattering. Somewhat surprisingly, this system could possibly be easier to treat than either the $e^{\pm}$-H_2 systems. Since the projectile is electrically neutral, the long range interactions fall off as $O(1/R^6)$, and so the nonspherical interactions of the H_2 molecule are mainly confined to short distances.

ACKNOWLEDGMENTS

This work was supported under the Australian Research Council's Discovery Program (Project No. 0665020).

[1] V. I. Kukulin and V. M. Krasnopol'sky, J. Phys. G **3**, 795 (1977).
[2] K. Varga and Y. Suzuki, Phys. Rev. C **52**, 2885 (1995).
[3] Y. Suzuki and K. Varga, *Stochastic Variational Approach to Quantum-Mechanical Few-Body Problems* (Springer, New York, 1998), Vol. 172.
[4] W. Cencek and J. Rychlewski, J. Chem. Phys. **98**, 1252 (1993).
[5] J. Komasa, W. Cencek, and J. Rychlewski, Phys. Rev. A **52**, 4500 (1995).
[6] K. Strasburger and H. Chojnacki, J. Chem. Phys. **108**, 3218 (1998).
[7] S. Bubin and L. Adamowicz, J. Chem. Phys. **120**, 6051 (2004).
[8] H. H. Sørensen, D. V. Fedorov, and A. S. Jensen, in *Nuclei and Mesoscopic Physics: Workshop on Nuclei and Mesoscopic Physics; WNMP 2004*, edited by V. Zelevinsky, AIP Conf. Proc. No. 777 (AIP, Melville, NY, 2005), pp. 12–20.
[9] G. G. Ryzhikh and J. Mitroy, Phys. Rev. Lett. **79**, 4124 (1997).
[10] G. G. Ryzhikh, J. Mitroy, and K. Varga, J. Phys. B **31**, 3965 (1998).
[11] S. F. Boys, Proc. R. Soc. London, Ser. A **258**, 402 (1960).
[12] K. Singer, Proc. R. Soc. London, Ser. A **258**, 412 (1960).
[13] I. A. Ivanov, J. Mitroy, and K. Varga, Phys. Rev. Lett. **87**, 063201 (2001).
[14] I. A. Ivanov, J. Mitroy, and K. Varga, Phys. Rev. A **65**, 022704 (2002).
[15] R. J. Drachman and S. K. Houston, Phys. Rev. A **12**, 885 (1975).
[16] F. E. Harris, Phys. Rev. Lett. **19**, 173 (1967).
[17] K. F. Canter, J. D. McNutt, and L. O. Roellig, Phys. Rev. A **12**, 375 (1975).
[18] J. B. Smith, J. D. McGervey, and A. J. Dahm, Phys. Rev. B **15**, 1378 (1977).
[19] P. G. Coleman, S. Rayner, F. M. Jacobsen, M. Charlton, and T. L. West, J. Phys. B **27**, 981 (1994).
[20] B. G. Duff and F. F. Heyman, Proc. Phys. Soc. London **517**, 281 (1962).
[21] R. Guérout, M. Jungen, and C. Jungen, J. Phys. B **37**, 3043 (2004).
[22] R. Guérout, M. Jungen, and C. Jungen, J. Phys. B **37**, 3057 (2004).
[23] I. A. Ivanov, J. Mitroy, and K. Varga, Phys. Rev. A **65**, 032703 (2002).
[24] D. W. Martin and P. A. Fraser, J. Phys. B **13**, 3383 (1980).
[25] J. Mitroy and M. W. J. Bromley, Phys. Rev. A **68**, 035201 (2003).
[26] T. C. Griffith and G. R. Heyland, Phys. Rep., Phys. Lett. **39**, 169 (1978).
[27] M. Charlton, Rep. Prog. Phys. **48**, 737 (1985).
[28] P. G. Coleman, T. C. Griffith, G. R. Heyland, and T. L. Killeen, J. Phys. B **8**, L185 (1975).
[29] P. A. Fraser, Adv. At. Mol. Phys. **4**, 63 (1968).
[30] R. A. Ferrell, Phys. Rev. **110**, 1355 (1958).
[31] J. Mitroy and I. A. Ivanov, Phys. Rev. A **65**, 012509 (2001).
[32] J. Mitroy, Aust. J. Phys. **48**, 646 (1995).
[33] A. K. Bhatia, A. Temkin, R. J. Drachman, and H. Eiserike, Phys. Rev. A **3**, 1328 (1971).
[34] T. F. O'Malley, Phys. Rev. **130**, 1020 (1963).
[35] T. F. O'Malley and R. W. Crompton, J. Phys. B **13**, 3451 (1980).
[36] Z. L. Petrovic, T. F. O'Malley, and R. W. Crompton, J. Phys. B **28**, 3309 (1995).
[37] A. K. Bhatia, A. Temkin, and H. Eiserike, Phys. Rev. A **9**, 219 (1974).
[38] J. Mitroy, Phys. Rev. A **66**, 022716 (2002).
[39] G. W. F. Drake, M. M. Cassar, and R. A. Nistor, Phys. Rev. A **65**, 054501 (2002).
[40] Z. C. Yan, J. F. Babb, A. Dalgarno, and G. W. F. Drake, Phys. Rev. A **54**, 2824 (1996).
[41] S. K. Houston and R. J. Drachman, Phys. Rev. A **3**, 1335

(1971).
[42] Y. K. Ho and P. A. Fraser, J. Phys. B **9**, 3213 (1976).
[43] P. Van Reeth and J. W. Humberston, J. Phys. B **32**, 3651 (1999).
[44] B. I. Campeanu and J. W. Humberston, J. Phys. B **10**, L153 (1977).
[45] P. van Reeth, J. W. Humberston, K. J. Iwata, R. J. Greaves, and C. M. Surko, J. Phys. B **29**, L465 (1996).
[46] S. Bubin and L. Adamowicz, Phys. Rev. A **74**, 052502 (2006).
[47] S. Chiesa, M. Mella, and G. Morosi, Phys. Rev. A **66**, 042502 (2002).
[48] J. E. Blackwood, M. T. McAlinden, and H. R. J. Walters, Phys. Rev. A **65**, 032517 (2002).
[49] P. Van Reeth and J. W. Humberston, J. Phys. B **93**, 133001 (2003).
[50] D. Bressanini, G. Morosi, and S. Tarasco, J. Chem. Phys. **123**, 204109 (2005).
[51] H. R. J. Walters, A. C. H. Yu, S. Sahoo, and S. Gilmore, Nucl. Instrum. Methods Phys. Res. B **221**, 149 (2004).
[52] A. Basu, P. K. Sinha, and A. S. Ghosh, Phys. Rev. A **63**, 052503 (2001).
[53] P. A. Fraser, J. Phys. B **1**, 1006 (1968).
[54] M. I. Barker and B. H. Bransden, J. Phys. B **1**, 1109 (1968).
[55] R. J. Drachman and S. K. Houston, J. Phys. B **3**, 1657 (1970).
[56] J. E. Blackwood, M. T. McAlinden, and H. R. J. Walters, J. Phys. B **35**, 2661 (2002).
[57] J. Mitroy, M. W. J. Bromley, and G. G. Ryzhikh, J. Phys. B **35**, R81 (2002).
[58] M. Charlton and J. W. Humberston, *Positron Physics* (Cambridge University Press, Cambridge, UK, 2001).
[59] R. A. Ferrell, Rev. Mod. Phys. **28**, 308 (1956).
[60] E. Boronski and R. M. Nieminen, Phys. Rev. B **34**, 3820 (1986).
[61] V. A. Dzuba, V. V. Flambaum, W. A. King, B. N. Miller, and O. P. Sushkov, Phys. Scr. **t46**, 248 (1993).
[62] J. Mitroy, Phys. Rev. A **72**, 062707 (2005).
[63] R. M. Nieminen, I. Välimaa, M. Manninen, and P. Hautojärvi, Phys. Rev. A **21**, 1677 (1980).
[64] K. Rytsola, J. Vettenranta, and P. Hautojarvi, J. Phys. B **17**, 3359 (1984).
[65] Y. Nagashima, T. Hyodo, K. Fujiwara, and A. Ichimura, J. Phys. B **31**, 329 (1998).
[66] J. P. Hernandez, Phys. Rev. A **14**, 1579 (1976).
[67] J. J. Engbrecht, M. J. Erickson, C. P. Johnson, A. J. Kolan, A. E. Legard, S. P. Lund, M. J. Nyflot, and J. D. Paulsen, Phys. Rev. A **77**, 012711 (2008).
[68] M. Skalsey, J. J. Engbrecht, C. M. Nakamura, R. S. Vallery, and D. W. Gidley, Phys. Rev. A **67**, 022504 (2003).
[69] S. K. Adhikari, P. K. Biswas, and R. A. Sultanov, Phys. Rev. A **59**, 4829 (1999).
[70] J. Di Rienzi and R. J. Drachman, Phys. Rev. A **70**, 052706 (2004).
[71] J. Mitroy and I. A. Ivanov, Phys. Rev. A **65**, 042705 (2002).
[72] R. S. Vallery, A. E. Leanhardt, M. Skalsey, and D. W. Gidley, J. Phys. B **33**, 1047 (2000).
[73] R. A. Fox, K. F. Canter, and M. Fishbein, Phys. Rev. A **15**, 1340 (1977).
[74] L. D. Landau and E. M. Lifshitz, *Quantum Mechanics (Non-Relativistic Theory)* (Pergamon, Oxford, 1977), Vol. 3.
[75] H. A. Bethe, Phys. Rev. **76**, 38 (1949).
[76] M. Fishbein and K. F. Canter, Phys. Lett. **55**, 398 (1975).
[77] B. R. Levy and J. B. Keller, J. Math. Phys. **4**, 54 (1963).
[78] R. P. Fontana and R. Bernstein, J. Chem. Phys. **41**, 1431 (1964).
[79] P. S. Ganas, Phys. Rev. A **5**, 1684 (1972).
[80] M. K. Ali and P. A. Fraser, J. Phys. B **10**, 3091 (1977).
[81] N. K. Sarkar and A. S. Ghosh, J. Phys. B **30**, 4591 (1997).